

The method for calculating the bearing capacity of cold-formed C-Section axial compression member using Direct Strength Method

An Myong Chol*¹ , Ju Su In¹ , Jang Yong Song¹ 

¹Faculty of Civil Engineering, Pyongyang University of Architecture, Pyongyang DPR Korea

*Corresponding Author: shypinguo202134@yeah.net

ARTICLE INFO

Article history:

Received 13-10-2023

Revised 21-11-2023

Accepted 28-11-2023

Available online 30-11-2023

E-ISSN: 2622-1640

P-ISSN: 2622-0008

How to cite:

Chol A. M, In J. S., Song J. Y. The method for calculating the bearing capacity of cold-formed C-Section axial compression member using Direct Strength Method. International Journal of Architecture and Urbanism. 2023. 7(3): 443-464.

ABSTRACT

The paper carried out numerical analysis using experimental and finite element analysis methods to determine the bearing capacity of cold-formed C-section axial compression member. Finite element analysis was performed using the application ABAQUS and the results were compared with experimental measurements. This paper also made out the reason for the error between the experimental results and the results of the finite element analysis, and the ultimate bearing capacity is determined by finite element analysis with C-section axial compression member of various sizes. At the same time, the effect of initial geometric imperfection on the bearing capacity of the member is analyzed in detail. Based on finding out that the supporting capacity of the member is directly related to local buckling, distortional buckling, and lateral-bending buckling critical stress, the formula for calculating the bearing capacity of the cold-formed C-section axial compression member by analyzing the research results on the direct strength method.

Keywords: buckling, CFS, DSM, experiment, steel



This work is licensed under a Creative Commons Attribution-ShareAlike 4.0 International.

1. Introduction

Research on the design method of cold-formed steel members using direct strength method has recently become an important research topic in the design of lightweight steel structural members. The direct strength method is a method of estimating the bearing capacity of a member directly from the critical stress at the elastic stage, which is easy to apply in practice and has a very little calculation process compared to the conventional effective section method. The successes of the direct strength method have already been reflected and used in the regulations and guidelines in various countries, including AISI, and further research is being carried out for its development. The focus of the direct strength method is to clarify the relationship between the confined slenderness and the bearing capacity of the members, and for this more and more research is required. In [7][8], study was carried out to evaluate the bearing capacity of cold-formed bending members, and in [9], a combination of experimental and numerical methods was carried out. In order to determine the bearing capacity of the cold-formed C-Section axial compression members, and supporting capacity was determined through the compression tests on the element of 200-600 mm. Using the finite element analysis method, the bearing capacity of the C-section axial compression member was determined and compared with the experimental values. The effect of initial geometric imperfection on the bearing

capacity was analyzed at the same time. Varying the length of C-section members of various sizes from 200 to 6000 mm, the analysis was carried out to determine the bearing capacity of the members and the results were formulated by regression analysis.

2. Method

Preparations of elements for an experiment

For the experiment of cold-formed steel structural member, the diagram is set up correctly and the experimental member is prepared. The diagram and the location of the measurement point for the compression experiment of the cold-formed steel structural member are defined (Figure 1,2 and Table 1).

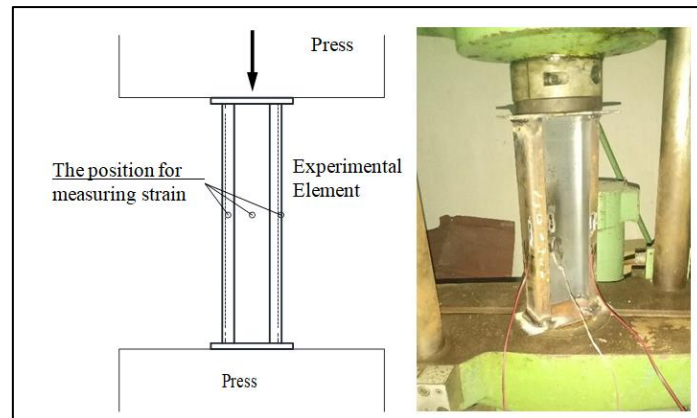


Figure 1 Diagram of pressing experiment of cold-formed C-Section member

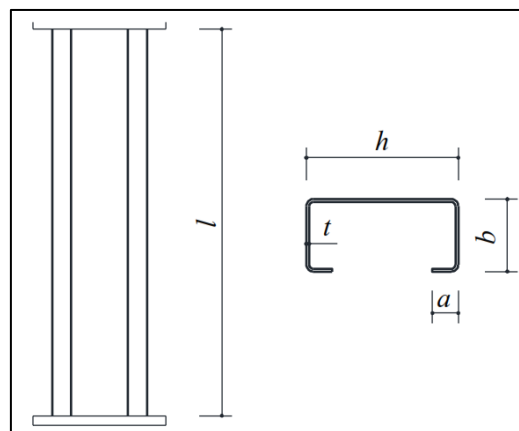


Figure 2 Geometric shape and dimension of experimental member

Table 1 The geometrical shape and size of test member

No	Symbol	h (mm)	b (mm)	a (mm)	t (mm)	l (mm)
1	C100-200	99	63	24	1.87	194
2	C100-300	99	63	24	1.93	291
3	C100-400	99	63	24	2	402
4	C110-200	109	51	19.5	1.85	198
5	C110-300	109	51	19.5	1.89	297
6	C110-400	109	51	19.5	1.85	376
7	C160-200	162.8	68.8	22.6	1.98	200
8	C160-300	162.8	68.8	22.6	2.02	302
9	C160-400	162.8	68.8	22.6	2.01	397

Experimental members are shown in Figure 3.



Figure 3 Experimental elements

Tensile experiments are done to obtain the physical properties of the experimental material. The specimen for tensile test is shown in figure 4 and table 2.

The measured values are as follows.

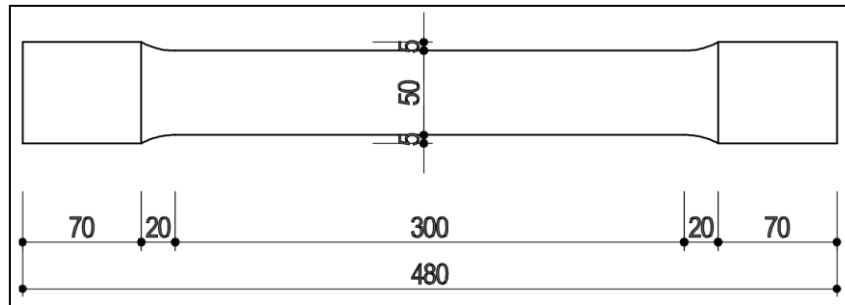


Figure 4 Dimension of the specimen for measuring the strength of the steel material

Table 2 Characteristics of the specimen through measurement

Numbers ofspecimen	Yield stress f_n (MPa)	Ultimate strength f_u (MPa)	Elasticity coefficient E (MPa)
4	371.3	498.7	202133

Make sure the dimensions of specimen and inspect everything carefully including welding joints, as there can be errors in the physical properties since some specimen may have imperfections, so experimental results should be analyzed by precisely determining the characteristics of the imperfections [1].

Pressing experiment of cold-formed buckling C-Section axial compression member

The strain measuring device is installed on the measuring point of the specimen and the computer for the record as well and they are connected to the press. The machine of the press is started to prepare for pressing, and pressing is done using a hydraulic device. Pressing speed should be 10 KN /min. Record the data with the units of 5 KN or 7.5 KN. Figure 5 shows the recording of the measured data in the experiment.

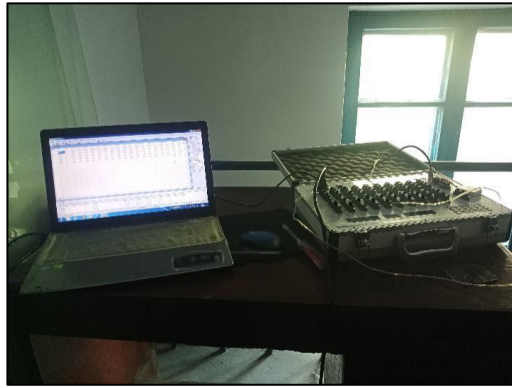


Figure 5 Strain measurement of experimental element by the measuring device

Strain measuring device is installed in a cross side at the center of the panel, the center of the flange and the lip [1] [4] because, in general, the strain in the middle part becomes the maximum, and at that time, loads are recorded by reading the figure displayed on the press, as shown in the member with strain measuring device in Figure 6.



Figure 6 Member with strain measuring device

If strain is measured, the stress in that part can be obtained, and according to the result, the relationship between the stress and the strains during the buckling process can be obtained, as nine members had been tested, where some specimens had local buckling and some members had restrained torsional buckling, and some of the results are shown in Figure 7 and table 6.



Figure 7 Members broken by buckling loss

The following figure shows the broken state of the member of the damage.



Figure 8 Broken state of the material with damage

As shown in Figure 8, the failure of the specimen with initial damage causes a loss of bearing capacity, starting with local buckling for relatively minor loading in the damaged part. Through the experiments it was proved that, as the load increases to a certain extent, the loss of stability begins to occur, and some parts of the steel plate that compose the member will lose the bearing capacity and become unable to pressurize the press with increasing out-of-plane displacement [4].

Analysis of the experiment results

The measurement results of the loads and strains applied on the experimental members are as follows:

Table 3 The measurement results of the loads and strains of the C110-300 element

No	Load(KN)	Strain (Center of the panel) $\times 10^{-3}$	Strain (Center of flange) $\times 10^{-3}$	Strain(Lip) $\times 10^{-3}$
1	7.5	0.001	0.001	0.002
2	15	0.08	0.176	0.03
3	22.5	0.143	0.31	0.066
4	30	0.224	0.464	0.095
5	37.5	0.301	0.597	0.157
6	45	0.379	0.712	0.214
7	52.5	0.556	0.952	0.346
8	60	0.656	1.104	0.432
9	67.5	0.715	1.191	0.48
10	75	0.841	1.335	0.564
11	82.5	0.971	1.435	0.638
12	94.8	1.066	1.501	0.712

Using the experimental results in Table 3, it is possible to evaluate in detail how big the bearing capacity of the member is and be able to know how much load is applied when entering the yield stress at the measurement point, as the bearing capacity of C110-300 is 94.8 KN, and the strain pattern is shown in Figure 7, which as you can see from the figure, local buckling occurs at the top of the panel and the blade and loses its bearing capacity at the location where the measurement point is located, suggesting that local buckling and restrained torsional buckling occur simultaneously, and looking at the strain of the measurement points in Table 3, it is clear that the strain at that location is in the elastic stage, indicating that the vertical strain in the middle part of the experimental member is not significant and the bearing capacity is determined by failure due to buckling, and the bearing capacity of members is determined in the same way as shown in Table 4.

Table 4 Supporting capacity of experimental members

No	Symbol	Result $P_{u,exp}$ (KN)
1	C100-200	113.8
2	C100-300	113.2
3	C100-400	114.8
4	C110-200	102.3
5	C110-300	94.8
6	C110-400	87.6
7	C160-200	102.5
8	C160-300	100.2
9	C160-400	110.1

The experimental data above are the basis for evaluating the bearing capacity of cold-formed C-section axial compression members; however, more experiments are necessary to determine the bearing capacity. Since this costs quite a lot of money, we should study combining with finite element analysis. In the next section, more detailed comparison and analysis of the results obtained in the experiments and those obtained by the finite element analysis will be done to verify the accuracy of the finite element analysis method and investigate the detailed method to determine the bearing capacity [5].

3. Research based on finite element analysis

Finite element analysis method of cold-formed C-Section axial compression member

Experiments are expensive, and the manufacture of various test members is often difficult to perform because of the unavailable size of the members. This disadvantage is addressed by the application of numerical methods based on finite element analysis. Using ABAQUS, a recently popular finite element analysis program, the behavior of cold-curved C-bar core compression members is investigated. First, to verify the practicability of finite element analysis, we analyze the finite element model as an experimental member and compare the results. At that time, physical characteristics of material for analysis and its method should be determined correctly. According to previous studies, the models for the physical properties of steel structural materials were used in various ways, and it is common to use ideal elastic-plastic models, two-linear models, and multi-linear models. We are not going to mention it further because it has been widely utilized in previous studies; we use the two-segment model in this essay. Cold-formed C steel center compression members must consider both material non-linearity and geometric non-linearity since the thickness of the individual slab elements forming the steel bars is very thin, and the bearing capacity is determined using the post-buckling strength. There are several such methods of nonlinear analysis, but it is useful to use Riks method to obtain accurate analysis results by considering both material non-linearity and geometric non-linearity simultaneously [6].

Modeling the finite element analysis of cold-formed C-section axial compression member considering initial geometric imperfection

Authors use S4R for the modeling of cold-formed C-section axial compression members, with the number of meshes of section ranging from 5 to 20 on one side. This degree of resolution ensures the accuracy of the analysis. At this time, the member shall be allowed to shift from both ends to the longitudinal axis for the axial compression member, while other displacements can be limited, and rotational displacements would be restricted. Unlike the experiments, the loading diagram is adopted at both ends, and boundary conditions are imposed to restrict the longitudinal displacement in the middle section.

The next important problem of FEM modeling is to accurately reflect the geometric error in the manufacturing stage, i.e., the difference between the standard size and the dimensions of the actual member. In general, this difference is estimated to depend on the thickness of the sheet, and the application of ABAQUS can be implemented using the Imperfection function. To use the Imperfection function, we perform the Buckle analysis of the member and take the method to give the difference according to the

template by the ratio of the thickness of the plate. Let us see the effect of such a difference on the actual bearing capacity. For example, let us consider a central compression member of cold-formed C-section (standard: C160X60X20X2). Since the effects of local buckling and confinement torsional buckling are all present when the length of the member is 800 mm, let us assume the length is 800 mm. The finite element analysis model developed in ABAQUS is shown in Figure 9.

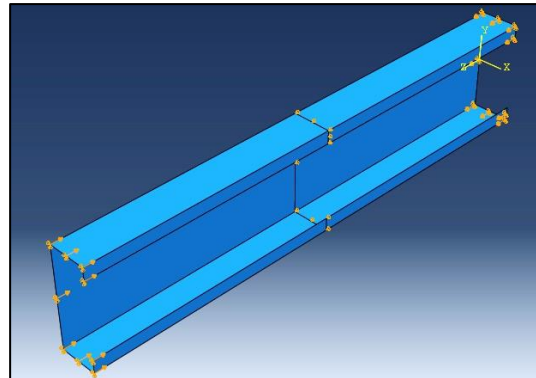


Figure 9 Analysis model

First, we do the analysis to obtain a vibrating mode and determine the imperfection patterns. The initial geometric imperfection patterns are shown in Figure 10.

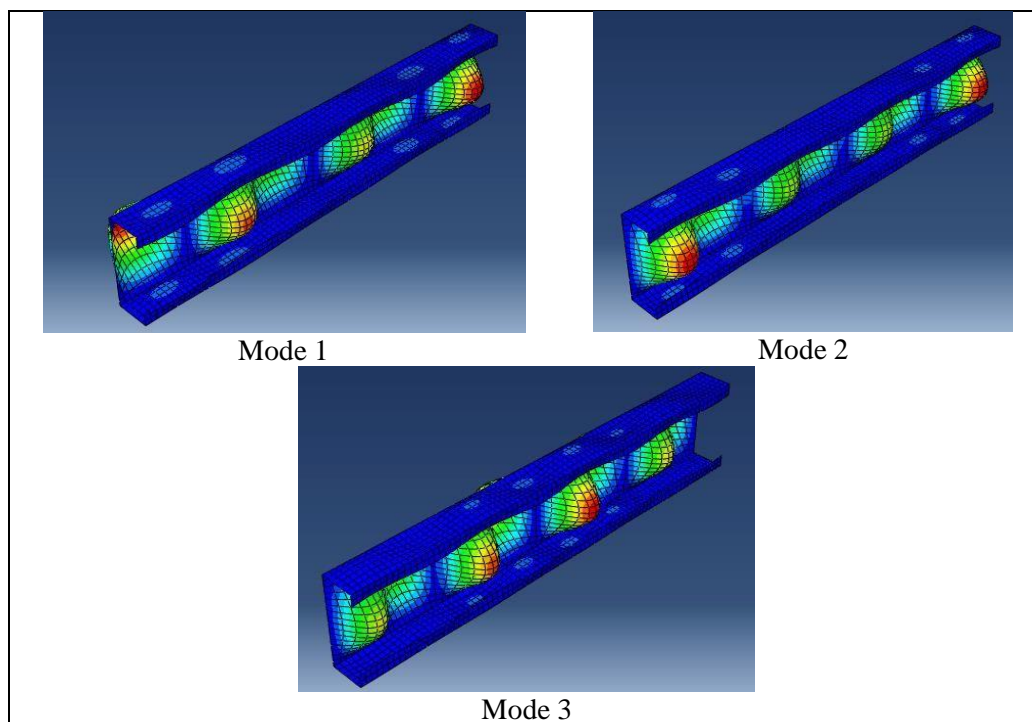


Figure 10 The Mode analysis results

Next, the initial geometric imperfection is input into the steel plate thickness ratio using the Imperfection function of the finite element analysis software ABAQUS, and a non-linear analysis of the elastic-plastic load is performed to determine the bearing capacity. At that time, the magnitude of the initial geometric imperfection was determined by applying 0.03, 0.3, 0.5, 1, 2, and 3 times the wall panel thickness to determine the bearing capacity. The analysis results are shown in Figure 11.

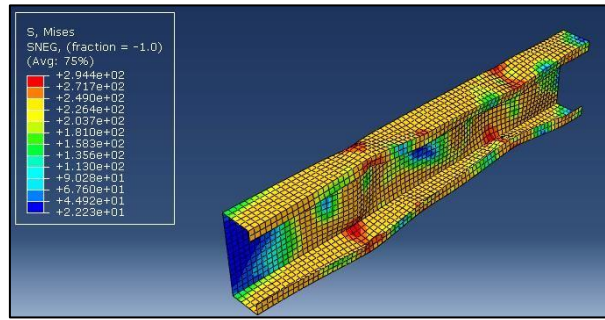


Figure 11 Analysis result when the imperfection is half of the plate thickness

The bearing capacity of the member with initial geometric imperfection is shown in Table 5.

Table 5 The change of the bearing capacity with initial geometric imperfection

The ratio of initial geometric imperfection to thickness of steel plate	The bearing capacity of the member(KN)	The proportion to the bearing capacity in no initial geometric imperfection (%)
0	114.7	100
0.03	111.7	97.42
0.3	111.3	97.05
0.5	112.7	98.31
1	105.1	91.66
2	90.2	78.68
3	90.1	78.53

As shown in Table 5, the effect of initial geometric imperfection on the bearing capacity is relatively large.

It describes that the initial geometric imperfection does not significantly affect up to 0.5 times the cold-formed C-section thickness, but at 2 and 3 times the thickness has a significant effect on the bearing capacity and decreases by approximately 20%. Regarding the dimensions of the experimental members, the difference between the dimensions and the actual dimensions is generally within the 0.5 times thickness range. Therefore, in the analysis, Imperfection estimates the bearing capacity considering 0.5 times the thickness.

Comparison of experimental results with finite element analysis results

The analysis model of the C110-400 experimental element is shown in Figure 12 and 13

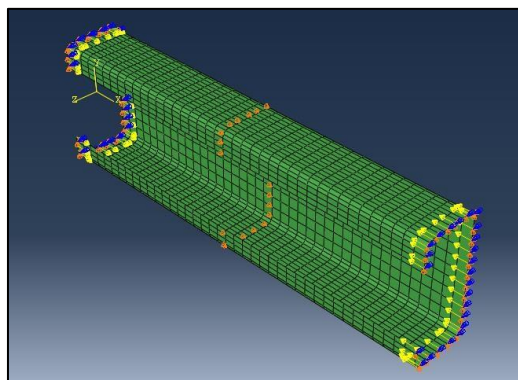


Figure 12 FEA analysis model of C110-400 experimental element

The analysis result is as the following if it is done in the same way above.

Imperfection was then given as the thickness of the plate.

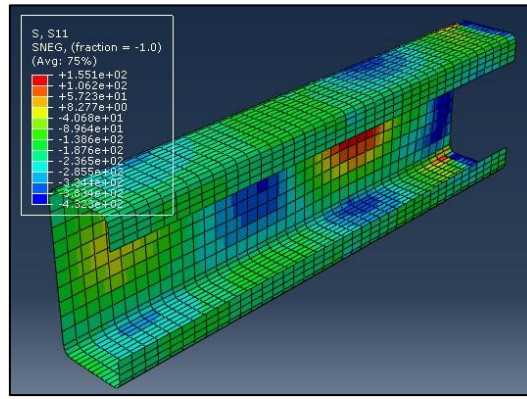


Figure 13 FEA analysis model of C110-400 experimental element (Stress distribution)

Let us now see the load-bearing characteristics of the experimental members. With the increase of the analysis step, the load changes as following.

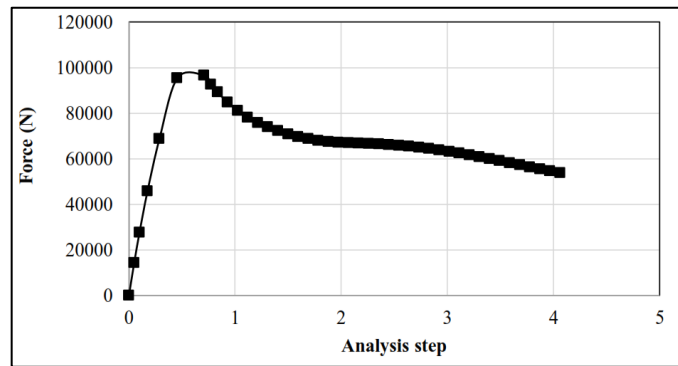


Figure 14 Changes of load according to the analysis process

As shown in Figure 14, the maximum bearing capacity of the experimental member is 95.4 KN.

In this way, the experimental members can be constructed by a finite element analysis model to determine the bearing capacity in an analytical way (Table 6).

Table 6 Calculation result of supporting capacity of element by ABAQUS

No	Symbol	Calculation result of supporting capacity based on experiments $P_{u,exp}$ (KN)	Calculation result of supporting capacity based on ABAQUS $P_{u,Abq}$ (KN)	Error between the experimental and analysis value (%) $\frac{P_{u,Abq} - P_{u,exp}}{P_{u,Abq}} \times 100$
1	C100-200	113.8	126.7	10.18
2	C100-300	113.2	124.6	9.14
3	C100-400	114.8	125.4	8.45
4	C110-200	102.3	112.5	9.06
5	C110-300	94.8	106.1	10.6
6	C110-400	87.6	95.4	8.17
7	C160-200	102.5	113.9	10.0
8	C160-300	95.5	116.3	17.88
9	C160-400	110.1	117.4	6.21

The error between the experimental values and the bearing capacity determined by finite element analysis is between 6.21% and 17.88%, as shown in Table 5. The reason for the large error of 17.88% in the C160-300

experimental member is due to the significant drop in bearing capacity caused by initial damage (Figure 8). Therefore, except for the experimental members C160-300, the range of error falls between 6.21% and 10.6%. This error is attributed to the uncertainty of measurement error and the boundary conditions of the experimental members during the experiment. In practice, various factors affect the manufacture and installation of actual members, but the analysis reflects ideal boundary conditions and material properties, ensuring the reliability of the analysis results despite some error in the experimental values.

Determination of the support capacity of cold-formed bending C-section Axial compression member by finite element analysis

Finite element analysis of cold-formed bending C-section axial compression members

The bearing capacity of the cold-formed C-section axial compression member can be determined by the analytical method presented in Section 4.1, which involves investigating the change of the bearing capacity curve with variations in the member length to develop a calculation formula that accounts for the influence of local buckling, restrained torsional buckling, and bending-torsional buckling on the bearing capacity. For example, let's examine the results of the analysis of steel bars of C220X75X20X2 in size. The analysis was conducted by varying the member length to 300, 400, 600, 900, 1200, 1800, 2400, 3000, 3600, 4200, 4800, 5400, and 6000 mm. Using the elastic-plastic load nonlinear analysis method with Riks' method, we need to consider changes step-by-step in the load-bearing characteristics. First, let's explore the variation in load-bearing characteristics when the member length is relatively short at 300 mm. The variation of the load-bearing capacity at different analysis stages is depicted in Figure 15.

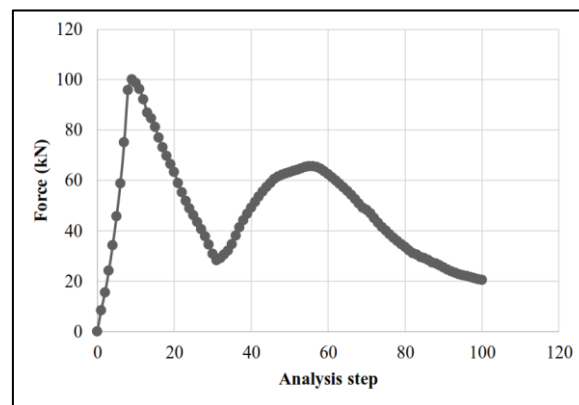


Figure 15 Changes of load-supporting capacity of C220X75X20X2 when its length is 300mm

As shown in Figure 16, the force that a member can sustain tends to increase to a certain degree and then decrease again according to the stage of analysis, after which it increases again to a certain degree and then loses its bearing capacity. This tendency of force to increase, decrease sharply, and then increase again is primarily attributed to the local buckling of some of the individual plates forming the cross-section. The resurgence of force is because some parts maintain their load-bearing capacity even after buckling, and these characteristics are particularly pronounced in thin-walled members. Now, let's examine the stress distribution at each stage of analysis in the following figure, with each stress distribution corresponding to an analytical step corresponding to the inflection points in the load-bearing capacity variation curve of Figure 16.

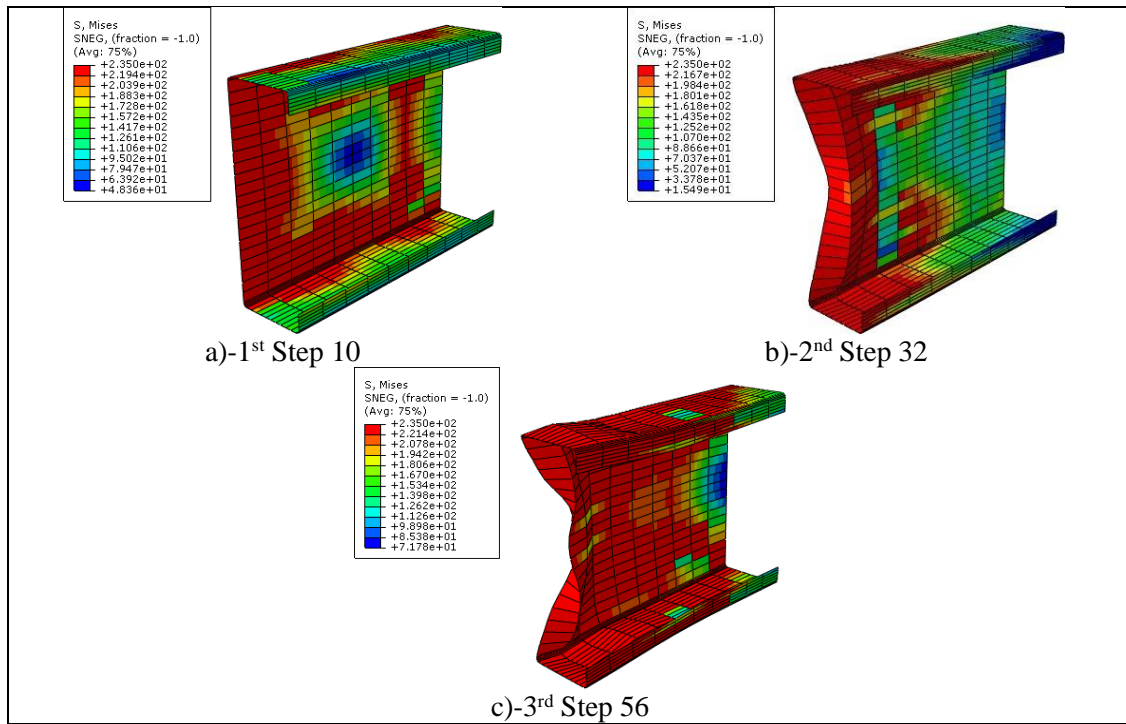


Figure 16 Stress according to analysis process of C220X75X20X2 when its length is 300mm

As shown in Figure 16a, at the stage of presenting the maximum load-bearing capacity, the overall area of the panel is red, with blue areas indicating that local buckling has already occurred. In Figure 16b, the red region extends over the wings, with some green or blue areas as well, and in Figure 16c, the wings are almost entirely red. At this time, the stress value of the red part in (c) is larger than that of the red part in (b).

As a result, as shown in step 10, local buckling occurred when the entire section reached a certain level of stress, but the shape of the section was maintained, and the load-carrying capacity was not lost. In step 32, however, the stress in some parts of the line was reduced by increasing the displacement of the panel, indicating a weakening of the load-carrying capacity. By stage 56, except for over-deformed parts, some sections will regain their load-bearing capacity to some extent.

This process occurs relatively quickly. Therefore, the bearing capacity of this member should be evaluated based on the load-bearing capacity of stage 10, which represents the maximum load. Next, let's examine the change in load-bearing characteristics when the member is 1200 mm long. The variation of the load-bearing capacity with the stage of analysis is shown in Figure 17.

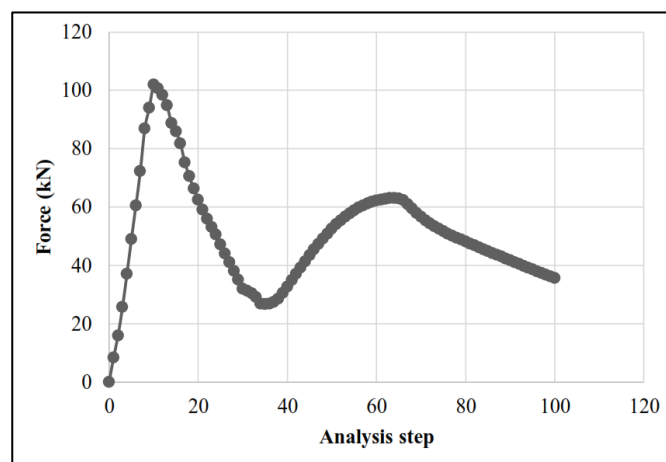


Figure 17 Changes in stress supporting capacity of C220X75X20X2 when its length is 200mm

As shown in Figure 18, there is some difference, although the variation is similar to relatively short lengths of members. Importantly, the load-bearing capacity rises to a certain extent, and the decreasing trend is relatively gradual. Furthermore, the value is relatively small, and the increase in load-bearing capacity is slower compared to when the load-bearing capacity increases to 300 mm. The stress distribution according to the analysis step is as follows.

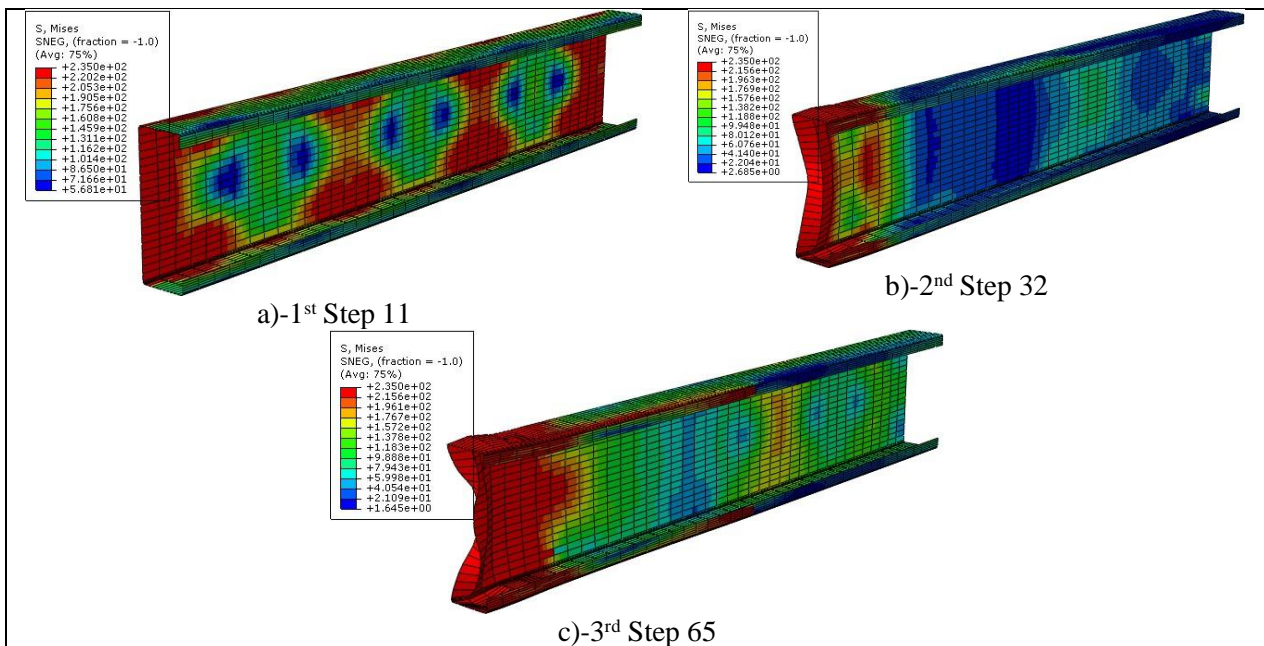


Figure 18 Stress according to analysis process of C220X75X20X2 when its length is 1200mm

As shown in Figure 18, the stress distribution in (a) is relatively regular, with restrained torsional buckling of the flange part at some distance in the middle of the panel, partial buckling in the panel, and local buckling on one end of the member in the panel. In (b), this leads to local buckling and a sudden drop in the load-bearing capacity. In (c), it shows that at one end of the member, the lip is retreating, creating a new balance and restoring a certain degree of bearing capacity. However, its bearing capacity remains relatively low. Thus, it is evident that as the length of the member increases, the second peak of the load-bearing capacity curve with the stage of analysis becomes slower and decreases.

Of course, the bearing capacity of a member must be based on the maximum peak of the bearing capacity curve. Next, let's examine the change in load-bearing characteristics when the length of the member is 6000 mm, which is relatively long.

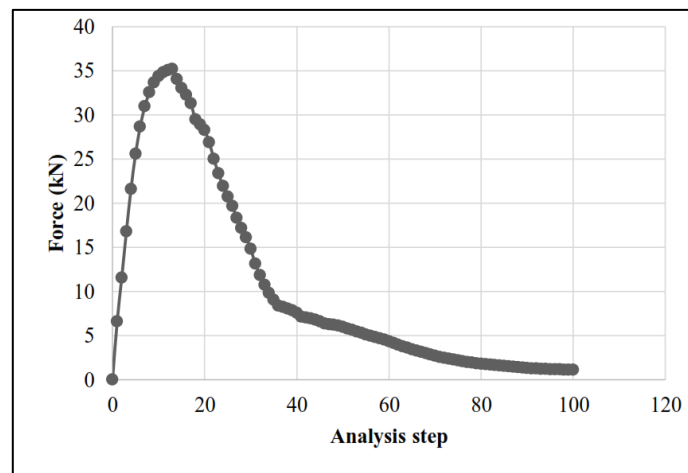


Figure 19 Changes in stress supporting capacity of C220X75X20X2 when its length is 6000mm

As shown in Figure 19, unlike the previous figures, the load-carrying capacity appears as a curve with a single peak. In other words, it indicates that there is no further upward trend after the load-bearing capacity of the member rises to a maximum value and then decreases. This means that as the length of the member increases, the peak of the second part gradually disappears. Now, let's examine the state of stress when the maximum load-bearing capacity point (step 14) is reached, as well as the state of stress after the curve has dropped rapidly (step 45).

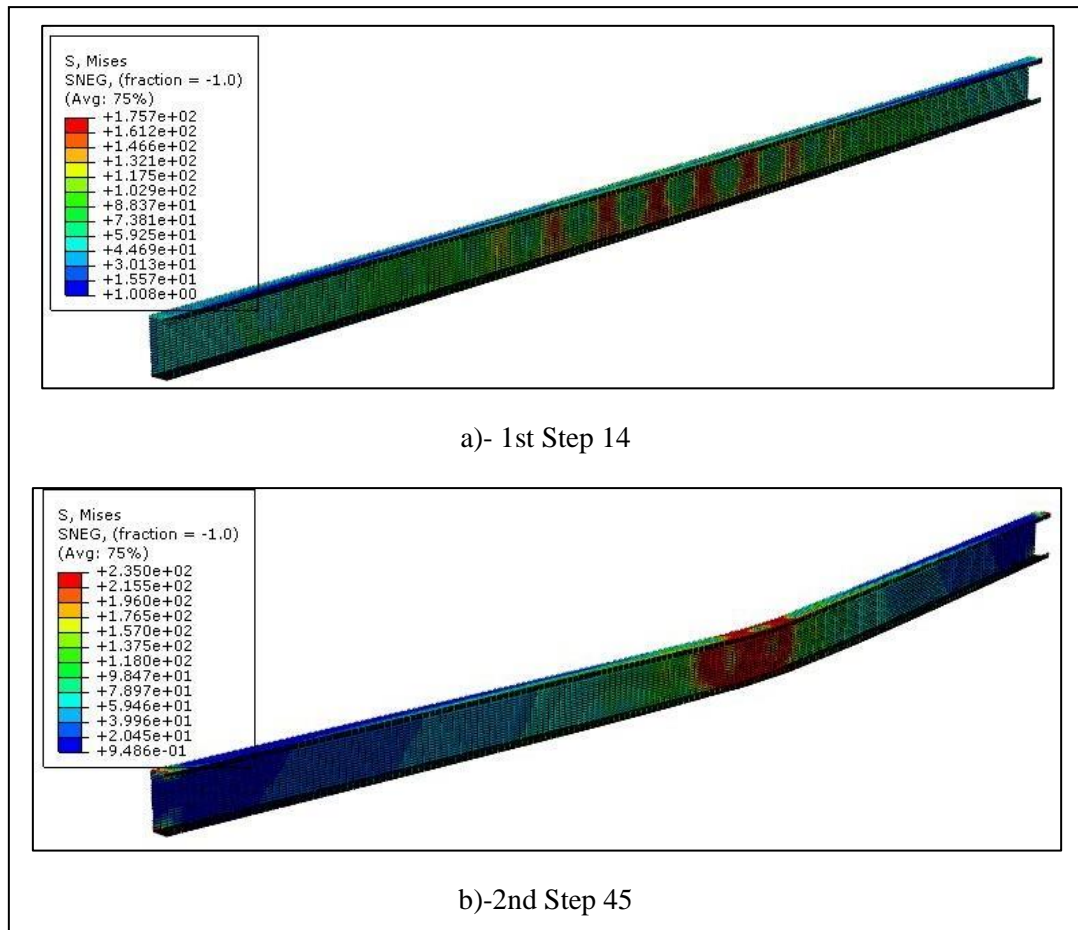


Figure 20 Stress according to analysis process of C220X75X20X2 when its length is 6000mm

As shown in Figure 20, the stress distribution at stage 14 is relatively uniform, with relatively high stress in the middle part of the member, and the maximum stress point does not reach the yield stress. This suggests that the failure of the member is due to the overall loss of stability. However, at stage 45, the stress in the middle part increases intensively, and the out-of-plane displacement increases, resulting in a complete loss of bearing capacity.

Through the above analysis, we can conclude that the bearing capacity of a member is influenced by local buckling when the length of the member is relatively short, by local buckling if the length is constant, and by restrained torsional buckling when the length is relatively long, ultimately affecting the mode of failure.

The supporting capability of cold-formed C-section axial compression members

The bearing capacity of cold-formed C-section axial compression members is considered in relation to the buckling critical stress at the elastic stage, which is determined using the program CUFSM written using the finite band method [3]. Details of the relationship between the ultimate stress at the elastic stage, the conditional slenderness, and the bearing capacity of the cold-formed C-section axial compression member are provided in Table 7.

Table 7 The relationship between the local buckling stress and supporting capacity of C-Section member

Section	$N_{u,Abq}$ (N)	N_{cr1} (N)	N_y (N)	$\frac{N_{u,Abq}}{N_y}$	$\lambda_1 = \sqrt{\frac{N_y}{N_{cr1}}}$
C100x50x15x2.5	104618	378166.58	135125	0.774	0.598
C100x50x20x2.5	110556	396724.2	141000	0.784	0.596
C120x50x15x2.5	116326	289073.06	146875	0.792	0.713
C120x60x15x2.5	124690	306763.54	158625	0.786	0.719
C140x50x20x2	79030.3	123295.2	131600	0.601	1.033
C140x50x20x2.2	95474.1	310080.54	144760	0.660	0.683
C140x50x20x2.5	117147	412175.05	164500	0.712	0.632
C140x50x20x3	149553	613083.66	197400	0.758	0.567
C160x60x20x2	85364.9	106600	150400	0.568	1.188
C160x60x20x2.2	99135.3	142054.18	165440	0.599	1.079
C160x60x20x2.5	122100	208772	188000	0.649	0.949
C160x60x20x3	168172	361285.44	225600	0.745	0.790
C180x70x20x2	94558.5	94137.804	169200	0.559	1.341
C180x70x20x2.2	107995	125427.97	186120	0.580	1.218
C180x70x20x2.5	135640	184281.92	211500	0.641	1.071
C200x70x20x2	89279.4	81234.12	178600	0.500	1.483
C200x70x20x2.2	108119	108157.92	196460	0.550	1.348
C200x70x20x2.5	134556	158760.2	223250	0.603	1.186
C220x75x20x2	93400.7	72494.47	192700	0.485	1.630
C220x75x20x2.2	111490	96549.277	211970	0.526	1.482
C250x75x20x2	93760.6	60758.72	206800	0.453	1.845
C250x75x20x2.2	113538	80820.643	227480	0.499	1.678
C250x75x20x2.5	132111	118432.6	258500	0.511	1.477

In the table, the bearing capacity of the member determined by $N_{u,Abq}$ finite element analysis, N_{cr1} - the local buckling critical load at the elastic stage, and N_y the bearing capacity when the entire section was considered to have entered the yield strength.

The value $N_{u,Abq}$ is the bearing capacity when the length of the member is taken as the length at which local buckling occurs.

The relationship between the conditional slenderness $\lambda_1 = \sqrt{\frac{N_y}{N_{cr1}}}$ and $\frac{N_{u,Abq}}{N_y}$ for taking into account the local buckling is plotted in Figure 21.

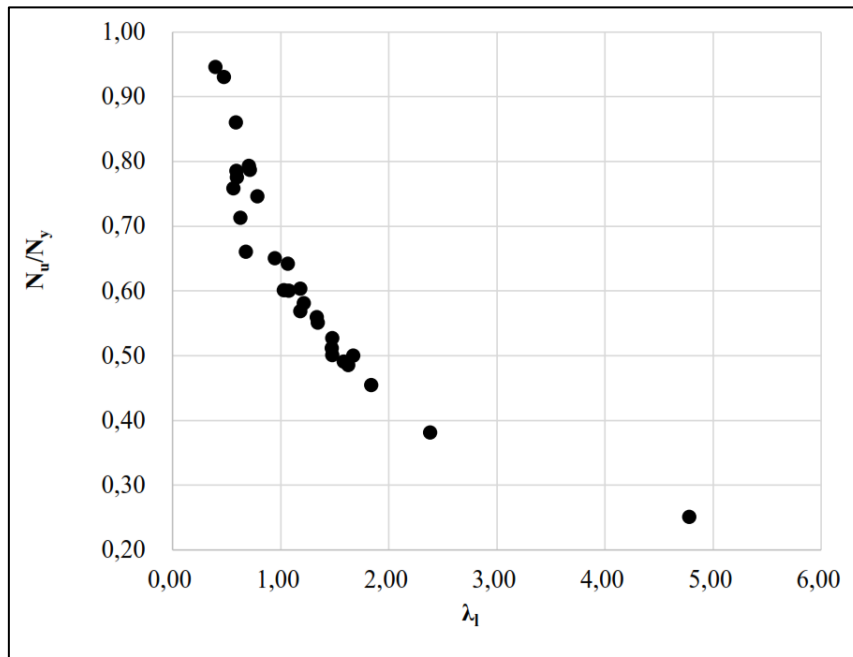


Figure 21 The relationship of $\frac{N_{u,Abq}}{N_y}$ λ_1

Table 8 The relationship between the lateral buckling stress and the bearing capacity of C-Section member

Section	$N_{u,Abq}$ (N)	N_{crd} (N)	N_y (N)	$\frac{N_{u,Abq}}{N_y}$	$\lambda_1 = \sqrt{\frac{N_y}{N_{crd}}}$
C100x50x15x2.5	107773	367428.16	135125	0.798	0.606
C100x50x20x2.5	110561	427781.7	141000	0.784	0.574
C120x50x15x2.5	116983	326744.38	146875	0.796	0.670
C120x60x15x2.5	127049	310139.89	158625	0.801	0.715
C140x50x20x2	84996.5	203363.61	131600	0.646	0.804
C140x50x20x2.2	98811.1	257396.52	144760	0.683	0.750
C140x50x20x2.5	119156	318641.75	164500	0.724	0.719
C140x50x20x3	152235	430586.1	197400	0.771	0.677
C160x60x20x2	93355	185110.08	150400	0.621	0.901
C160x60x20x2.2	99475	227866.85	165440	0.601	0.852
C160x60x20x2.5	129156	302071.6	188000	0.687	0.789
C160x60x20x3	170351	454332.48	225600	0.755	0.705
C180x70x20x2	97339.5	167260.32	169200	0.575	1.006
C180x70x20x2.2	114344	205921.19	186120	0.614	0.951
C180x70x20x2.5	139009	272912.4	211500	0.657	0.880
C200x70x20x2	98165.3	147386.8	178600	0.550	1.101

Section	$N_{u,Abq}$ (N)	N_{crd} (N)	N_y (N)	$\frac{N_{u,Abq}}{N_y}$	$\lambda_1 = \sqrt{\frac{N_y}{N_{crd}}}$
C200x70x20x2.2	111823	181594.25	196460	0.569	1.040
C200x70x20x2.5	137850	240944.7	223250	0.617	0.963
C220x75x20x2	99052.9	132279.57	192700	0.514	1.207
C220x75x20x2.2	116386	163041.06	211970	0.549	1.140
C250x75x20x2	94954.9	-	206800	0.459	-
C250x75x20x2.2	114938	-	227480	0.505	-
C250x75x20x2.5	134898	-	258500	0.522	-

In the table 8, the bearing capacity of the member is $N_{u,Abq}$, finite element analysis is N_{crd} - the local buckling critical load at the elastic stage is N_y the bearing capacity when the entire section was considered to have entered the yield strength.

At this time, the figure $N_{u,Abq}$ is the bearing capability of the member of the maximum taking into account the state of buckling. In the same way above, the relationship between $\lambda_1 = \sqrt{\frac{N_y}{N_{crd}}}$ and $\frac{N_{u,Abq}}{N_y}$ is as the following Figure 22.

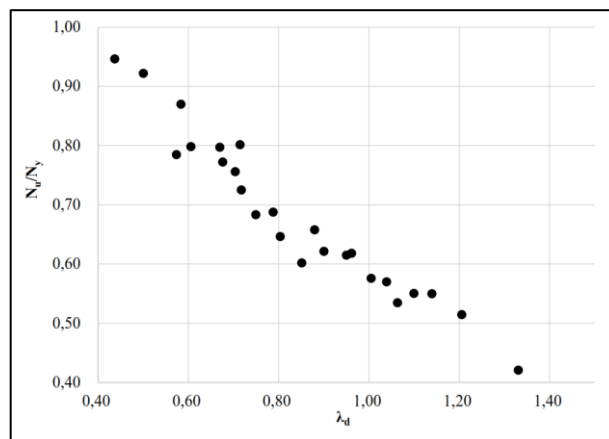


Figure 22 The relationship of $\frac{N_{u,Abq}}{N_y}$ λ_1

Figure 21 and Figure 22 show the relationship between the conditional ratio and member and also they have a certain relationship.

4. Calculation formula of cold-formed C-Section center suppression member

Mathematical modeling

Let's create a mathematical model of the curve line depicting the relationship between the conditional ratio and bearing capacity, as shown in Figure 22 and 23. To accomplish this, we need to utilize the formula provided in [2]. The bearing capacity, taking into account local buckling, is as follows.

$$N_{nl} = \left(1 - A \cdot \left(\frac{N_{cr1}}{N_y} \right)^B \right) \left(\frac{N_{cr1}}{N_y} \right)^B N_y \tag{1}$$

In the equation, change the value of B in the range of 0.3, 0.35, 0.4, 0.45, 0.5, 0.55, 0.6, 0.65 using the double way to determine the coefficient A and analyze the error according to the changing value of B, and as a result we can make out the formula.

The constant value of B in the equation is because the shape of the change curve of the conditioned ratio and bearing capacity do not change significantly.

IF we calculate A by applying the minimum squares method, it is as the following.

$$A = \frac{\sum \left[\left(\frac{N_{cr1}}{N_y} \right)^B - \left(\frac{N_{u,Abq}}{N_y} \right) \right]}{\sum \left[\left(\left(\frac{N_{cr1}}{N_y} \right)^B \right)^2 \right]} \tag{2}$$

Calculating A according to B using equation 2, yields the results of (A, B)-(0.360, 0.3), (0.379, 0.35), (0.281, 0.4), (0.368, 0.45), (0.333, 0.5), (0.281, 0.55), (0.258, 0.6).

The square root of the error is as the following.

$$\Delta^2 = \sum \left[\left[\left(1 - A \cdot \left(\frac{N_{cr1}}{N_y} \right)^B \right) \left(\frac{N_{cr1}}{N_y} \right)^B - \left(\frac{N_{u,Abq}}{N_y} \right) \right]^2 \right] \tag{3}$$

As a result of the calculations (0.333, 0.5), it was minimized as $\Delta^2 = 0.23$.

Therefore, the bearing capacity calculation considering the local buckling in the axial compression member is

$$N_{nl} = \left[1 - 0.333 \cdot \left(\frac{N_{cr1}}{N_y} \right)^{0.5} \right] \left(\frac{N_{cr1}}{N_y} \right)^{0.5} N_y \tag{4}$$

The variation of equation 4 has an extreme value of 0.666, and the resulting value is 0.75. That is, the above equation has meaning for the case of $\lambda_1 > 0.666$ and does not have meaning for smaller cases.

As shown in Figure. 22, for a certain small value of λ_1 , the bearing capacity reaches the value of the load, i.e. N_y that can be sustained when the entire section reaches the yield strength. Specifically in the interval $\lambda_1 < 0.4$.

In addition, the variation of the curve can be estimated by interpolating it by assuming that the curvature changes abruptly when reaching the extreme, and therefore it is not available in some regions, so that it changes linearly in the region of $0.4 \leq \lambda_1 \leq 0.8$.

Therefore, the relationship between the λ_1 -value and the bearing capacity is divided into three separate equations.

That is,

When $\lambda_1 < 0.4$

$$N_{nl} = N_y \quad (5-7)$$

And when $0.4 \leq \lambda_1 \leq 0.8$

$$N_{nl} = \left[1.27 - 0.676 \left(\frac{N_y}{N_{cr1}} \right)^{0.5} \right] N_y \quad (5-L)$$

$\lambda_1 > 0.8$

$$N_{nl} = \left[1 - 0.333 \cdot \left(\frac{N_{cr1}}{N_y} \right)^{0.5} \right] \left(\frac{N_{cr1}}{N_y} \right)^{0.5} N_y \quad (5-C)$$

In the equation $\lambda_1 = \sqrt{\frac{N_y}{N_{cr1}}}$

Let us model the bearing capacity calculation with respect to restrained distortional buckling as equation 6.

$$N_{nd} = \left[C + D \cdot \left(\frac{N_{crd}}{N_y} \right)^E \right] \left(\frac{N_{crd}}{N_y} \right)^E N_y \quad (6)$$

Let us determine C, D using the least squares method by varying the value of E in the range of 0.3, 0.35, 0.4, 0.45, 0.5, 0.55, 0.6, and 0.65, as previously applied.

Taking the value of E as a constant and applying the least squares method in detail, we have the following one.

Let $\left(\frac{N_{crd}}{N_y} \right)^E = x$, $\frac{N_{u,Abq}}{N_y} = y$, the above expression is denoted $y = Cx + Dx^2$.

The sum of the squares of the errors is defined as $f = \sum (y - y_i)^2$, and the value of the partial derivative must be zero, respectively, in order to minimize this value.

$$\begin{aligned} \frac{\partial f}{\partial C} &= 2 \sum (Cx_i + Dx_i^2 - y_i) x_i = 0 \\ \frac{\partial f}{\partial D} &= 2 \sum (Cx_i + Dx_i^2 - y_i) x_i^2 = 0 \end{aligned} \quad (7)$$

Therefore, C, D can be obtained by solving the following equation :

$$\begin{aligned} C \sum x_i^2 + D \sum x_i^3 - \sum x_i y_i &= 0 \\ C \sum x_i^3 + D \sum x_i^4 - \sum x_i^2 y_i &= 0 \end{aligned} \quad (8)$$

The calculation result is as the following (Table 9).

Table 9 Coefficients

No	C	D	E
1	0.3797	0.1914	0.3
2	0.4924	0.07942	0.35
3	0.5744	-0.00164	0.4
4	0.6355	-0.06151	0.45
5	0.6815	-0.10621	0.5
6	0.7164	-0.1397	0.55
7	0.7427	-0.16467	0.6

Based on the results calculated in the above table, the error for $C=0.7427$, $D=-0.16467$ and $E=0.6$ is minimized by $\Delta^2 = 0.0185$

Putting the result in a theorem, we have,

$$N_{nd} = 0.743 \left[1 - 0.222 \cdot \left(\frac{N_{crd}}{N_y} \right)^{0.6} \right] \left(\frac{N_{crd}}{N_y} \right)^{0.6} N_y \tag{9}$$

The above expression makes sense when $\lambda_d \geq 0.677$

For values smaller than this, the model is divided into straight sections.

From the results of the calculations, the value of $\lambda_d < 0.4$ is almost equal to the value of the bearing capacity when the shear surface reaches the yield strength, so the following relationship is proposed.

When $\lambda_d < 0.4$

$$N_{nd} = N_y \tag{10-Г)$$

When $0.4 \leq \lambda_d \leq 0.677$

$$N_{nd} = \left[1.339 - 0.848 \left(\frac{N_y}{N_{crd}} \right)^{0.5} \right] N_y \tag{10-Л)$$

When $\lambda_d > 0.677$

$$N_{nd} = 0.743 \left[1 - 0.222 \left(\frac{N_{crd}}{N_y} \right)^{0.6} \right] \left(\frac{N_{crd}}{N_y} \right)^{0.6} N_y \tag{10-Ц)$$

The equation indicates: $\lambda_d = \sqrt{\frac{N_y}{N_{crd}}}$

Validation of the calculation formula

In order to apply the calculation formula to practice, it is necessary to verify its significance.

A comparison of the analysis results and the newly proposed formula is shown in Figure 23 and Figure 24.

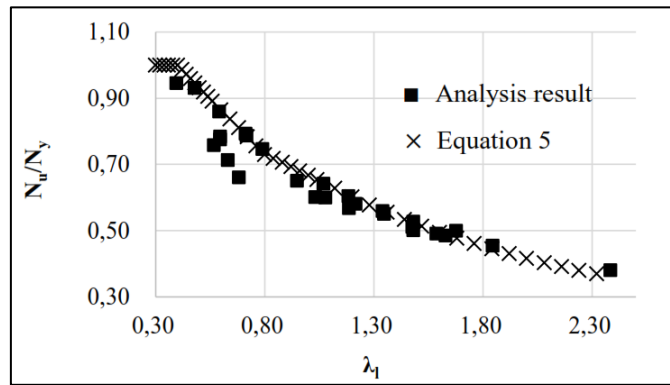


Figure 23 Comparison of results of analysis and equation 5.

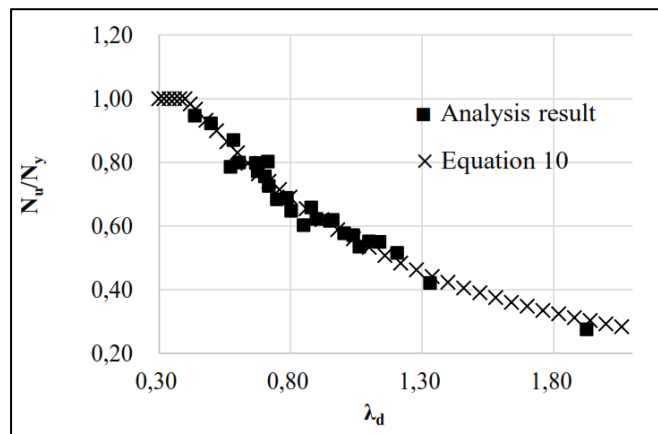


Figure 24 Comparison of results of analysis and equation 10

Since the newly proposed equation is a nonlinear function, the test of such a function should be performed by comparing the estimates according to the newly proposed equation and the sample values by finite element analysis to test hypotheses to investigate whether or not there is a difference.

First, let us perform a significance test for the proposed equation 5 considering the local buckling. First, we establish the statistical hypothesis that the “estimate X = sample Y”.

If the hypothesis is correct, we see that $Z = X - Y$ follows a normal distribution with mean zero and variance

$$\sigma_z^2.$$

Therefore, the test quantity $T = \frac{\mu_z}{\sigma_z}$ follows a normal distribution with mean 0 and variance 1 when the hypothesis is true.

When the significance level is 0.05, the test value according to the standard normal distribution function is $-\Phi(0.05) = 1.644$.

We would be able to get the standard normal through 29 analysis. The result is as the following.

$$T = \frac{\mu_z}{\sigma_z} = \frac{-0.027}{0.048} = -0.572$$

That is, since the absolute value of the test quantity is less than the test value, it enters the tolerance region.

Likewise, a significance test is performed for the newly proposed equation considering restrained distortional buckling.

$$T = \frac{\mu_z}{\sigma_z} = \frac{-0.003}{0.029} = -0.117$$

Through the analysis of 26 samples, the test quantity is found to be $T = \frac{\mu_z}{\sigma_z} = \frac{-0.003}{0.029} = -0.117$ which enters the feasible region.

Thus, when the significance level is 5%, the new expression is used as a result of the significance test for the equations considering both local and restrained torsional buckling, since the new hypothesis is acceptable.

5. Conclusion

The paper studied on the formula to calculate the strength of cold-formed C-Section axial compression member.

The result is that, the bearing capacity of the member depends on the conditional ratio and the relationship is as the following.

In the case of considering local buckling, when the conditional slenderness ratio is $\lambda_1 < 0.4$, since the total member section enters the yield stress, the bearing capacity of the member is determined by the load N_y at which the entire section can be loaded, and when $0.4 \leq \lambda_1 \leq 0.8$, it changes in a relatively linear relationship.

If $\lambda_1 > 0.8$, it has the shape of a curved line.

A similar phenomenon is observed for the restrained torsional buckling, where the linear interval is estimated to be smaller $\leq \lambda_d \leq 0.677$ for the local buckling.

Like this, if we estimate the supporting capacity of the member by using the Direct Strength Method, we can directly determine from the limited stress in an elastic stage.

But in practice, we use a lot of cold-formed bending steel bars so every factor needs to be made clear according to their section types.

6. Acknowledgement

Thank for evaluations given good ideas for the improvement of the work.

References

- [1] Cao Hung Pham, Gregory J. Hancock, «Numerical simulation of high strength cold-formed purlins in combined bending and shear», *Journal of Constructional Steel Research* 66 (2010) 1205–1217
- [2] B. W. Schafer, M.ASCE, «Local, Distortional, and Euler Buckling of Thin-Walled Columns», *JOURNAL OF STRUCTURAL ENGINEERING / MARCH 2002 / 289-299*
- [3] Demao Yang, Gregory J. Hancock, «Compression Tests of High Strength Steel Channel Columns with Interaction between Local and Distortional Buckling», *JOURNAL OF STRUCTURAL ENGINEERING, ASCE / DECEMBER 2004/1954-1963*
- [4] André Dias Martins, «Local-distortional interaction in cold-formed steel beams: Behaviour, strength and DSM design», *Thin-Walled Structures* 119 (2017) 879–901
- [5] Cao Hung Pham, Gregory J. Hancock, «Direct Strength Design of Cold-Formed C-Sections for Shear and Combined Actions» *JOURNAL OF STRUCTURAL ENGINEERING ASCE / JUNE 2012 / 759~769*

- [6] Ziqi He, Xuhong Zhou, Zhanke Liu, Ming Chen, «Post-buckling behaviour and DSM design of web-stiffened lipped channel columns with distortional and local mode interaction», *Thin-Walled Structures* 84 (2014) 189–203
- [7] Yan Lu, Tianhua Zhou, Wenchao Li, Hanheng Wu, «Experimental investigation and a novel direct strength method for cold-formed built-up I-section columns», *Thin-Walled Structures* 112 (2017) 125–139
- [8] Poologanathan Keerthan, Mahen Mahendran, «Experimental investigation and design of lipped channel beams in shear», *Thin-Walled Structures* 86 (2015) 174–184
- [9] Lorenzo Bertocchia, Daniele Comparinia, Giovanni Lavacchinib, Maurizio Orlandoc, Luca Salvatoric, Paolo Spinellid, «Experimental, numerical, and regulatory P-Mx-My domains for cold-formed perforated steel uprights of pallet-racks», *Thin-Walled Structures* 119 (2017) 151–165